Article

A One-Pot Approach to Hierarchically Nanoporous Titania Hollow Microspheres with High Photocatalytic Activity

Jiaguo Yu, Wen Liu, and Huogen Yu

Cryst. Growth Des., **2008**, 8 (3), 930-934• DOI: 10.1021/cg700794y • Publication Date (Web): 19 January 2008

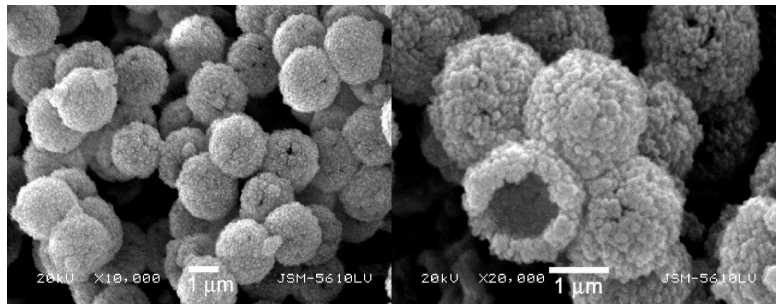

More About This Article

Additional resources and features associated with this article are available within the HTML version:

- Supporting Information
- Links to the 3 articles that cite this article, as of the time of this article download
- Access to high resolution figures
- Links to articles and content related to this article
- Copyright permission to reproduce figures and/or text from this article

View the Full Text HTML

CRYSTAL GROWTH & DESIGN
2008
VOL. 8, NO. 3
930–934

A One-Pot Approach to Hierarchically Nanoporous Titania Hollow Microspheres with High Photocatalytic Activity

Jiaguo Yu,* Wen Liu, and Huogen Yu

State Key Laboratory of Advanced Technology for Materials Synthesis and Processing, Wuhan University of Technology, Luoshi Road 122#, Wuhan, 430070, P. R. China

Received August 22, 2007; Revised Manuscript Received October 19, 2007

ABSTRACT: A simple one-step template method for the fabrication of crystalline titania (TiO_2) hollow microspheres, based on template-directed deposition and in situ template-sacrificial dissolution, is developed in pure water by using SiO_2 microspheres as templates and TiF_4 as the precursor at 60 °C. The wall thickness and size of the TiO_2 hollow spheres can be controlled by adjusting the concentration of the precursor TiF_4 and the size of the SiO_2 spheres, respectively. The prepared TiO_2 hollow spheres exhibit hierarchically nanoporous structures and a high photocatalytic activity. This hierarchically micromeso-macrostructured TiO_2 hollow microspheres should find various potential applications in photocatalysis, catalysis, solar cells, and separation and purification processes.

1. Introduction

Recently, there has been considerable interest in the synthesis of micrometer- and nanometer-sized hollow spheres because of their widespread potential applications in catalysis, drug delivery, chromatography separation, chemical reactors, controlled release of various substances, and protection of environmentally sensitive biological molecules.[1–3] Numerous chemical and physicochemical methods, such as the Kirkendall effect, Ostwald ripening, self-assembly techniques, template-sacrificial techniques, and chemically induced self-transformation,[4–9] have been developed to fabricate various hollow spheres. Among them, the template-directed synthetic method has proved to be the most effective route to produce inorganic hollow structures, and various templates, such as hard templates (e.g., polymer latex, carbon, and anodic aluminum oxide templates) and soft templates (e.g., supramolecular, ionic liquids, surfactant, and organogel), have been extensively employed.[10]

Titania (TiO_2) is a very important multifunctional material because of its peculiar and fascinating physicochemical properties and a wide variety of potential uses in diverse fields such as solar energy conversion, environmental purification, and water treatment. In particular, TiO_2 hollow structured materials have received more and more attention owing to their low density, high specific surface areas, and good photocatalytic activity.[11] Moreover, the hollow structured materials have also been considered as potential candidates for electrode materials in photochemical solar cells. It was reported that such materials were expected to exhibit a high light-collection efficiency and a fast motion of charge carriers because of their hollow structures, closely packed interpenetrating networks, and large internal surface area.[12] Although TiO_2 hollow spheres can be readily prepared by using a template method, one-step low-temperature synthetic routes to hierarchically nanoporous anatase hollow microspheres are less common, even though the increased surface area, light weight, and chemical accessibility associated with such materials offer distinct advantages. For example, Xia et al.[2] have reported the fabrication of amorphous TiO_2 mesoscale hollow spheres by templating their sol–gel precursor solutions on crystalline arrays of polystyrene particles and subsequently dissolving the polystyrene beads in toluene. Li et al.[6b] have reported the fabrication of TiO_2 and other metal oxide hollow spheres by using carbonaceous polysaccharide microspheres as templates and subsequently removing the templates by calcination. Caruso et al.[1] have successfully fabricated TiO_2 and inorganic hollow spheres by a layer-by-layer (LBL) approach, in which the composite organic–inorganic particles were first formed on the basis of the LBL technique, and the hybrid core–shell particles were calcined to create well-defined hollow spheres. Although the above methods have provided effective routes to prepare TiO_2 hollow spheres, postsynthetic removal of the template to produce the TiO_2 replica requires additional processing steps that can be costly, wasteful, and of environmental concern and thus limit the application of the template-directed approach. Clearly, these problems would be easily solved if the deposition of the inorganic phase could couple with the dissolution of the core in the same reaction medium.

In this work, we develop a simple one-step low-temperature template approach for the fabrication of hierarchically nanoporous TiO_2 hollow microspheres in pure water by using SiO_2 microspheres as templates and TiF_4 as the precursor at 60 °C. The preparation conditions are much milder and simpler than those of conventional methods, which require high-temperature calcination and etching procedures. Another advantage is that our products show an interesting hierarchically nanoporous spherical structure without using organic templates as porogens. Hierarchically structured porous materials are of great interest to catalysis, where an accurately controlled pore texture at different length scales can help reduce or otherwise control transport limitations.[13–16] In addition, experimental and theoretical investigations have demonstrated that the catalytic process would occur more efficiently in materials with a hierarchical pore size distribution on the nanoscale.[13,16,17] Thus, it is expected that the photocatalytic efficiency should be greatly enhanced for a hierarchically nanoporous material. We and other groups have proven that hierarchically nanoporous TiO_2 shows greatly enhanced photocatalytic activity.[13,16]

2. Experimental Section

2.1. Preparation of SiO_2 Template Microspheres. Monodisperse SiO_2 microspheres are synthesized by a modification of the Stober method, as described in our previous work.[18] In a typical synthesis, 8 mL of tetraethoxysilane is added dropwise to a mixed solution of dodecylamine (1.2 g), ethanol (160 mL), and water (100 mL) under

* Corresponding author. E-mail: jiaguoyu@yahoo.com.

10.1021/cg700794y CCC: $40.75
Published on Web 01/19/2008

stirring at about 10 °C. After 4 h, the white precipitates are filtrated, washed with ethanol and water three times, and dried in a vacuum oven at 60 °C for 8 h. The scanning electron microscope (SEM) image (Figure S1a) of the prepared SiO_2 microspheres indicates that the SiO_2 microspheres have smooth surfaces and uniform sizes with an average diameter of about 1.5 μm, similar to the results in our previous report.[18] The corresponding transmission electron microscope (TEM) image (Figure S1b) further confirms that the SiO_2 microspheres are solid and appear monodisperse.

2.2. Preparation of TiO_2 Hollow Spheres. TiF_4 (Aldrich) is used as the precursor for the preparation of TiO_2 hollow spheres. In a typical synthesis, theTiF_4 powder is dissolved in distillated water to prepare the precursor solution with a concentration of 0.01–0.1 M. Subsequently, 0.01 g of the SiO_2 microspheres is added into a 40 mL TiF_4 solution, which is then maintained at 60 °C for 12 h. After reaction, the powder precipitates are filtered, rinsed with distilled water and ethanol three times, and dried in a vacuum oven at 60 °C for 8 h. A series of experiments with varying reaction times are also carried out to get more evidence about the formation mechanism of the TiO_2 hollow spheres.

2.3. Characterization. The morphology observation is performed on a JSM-5610LV SEM (JEOL, Japan) at an accelerating voltage of 20 kV and a S4800 field emission SEM (FESEM, Hitachi, Japan), which is linked with an Oxford Instruments X-ray analysis system, at an accelerating voltage of 5 kV. X-ray diffraction (XRD) patterns are obtained on a D/MAX-RB X-ray diffractometer (Rigaku, Japan) using Cu Kα irradiation at a scan rate (2θ) of $0.05°\cdot s^{-1}$ and are used to determine the phase structures of the obtained samples. The accelerating voltage and applied current are 15 kV and 20 mA, respectively. X-ray photoelectron spectroscopy (XPS) measurements are done on a VG ESCALAB MKII XPS system with a MgKα source and a charge neutralizer. All the binding energies are referenced to the C1s peak at 284.8 eV of the surface adventitious carbon. TEM analyses are conducted with a JEM-2100F electron microscope (JEOL, Japan), using a 200 kV accelerating voltage. UV–visible spectra are obtained on an UV–visible spectrophotometer (UV-2550, Shimadzu, Japan). $BaSO_4$ is used as a reflectance standard in the UV–visible diffuse reflectance experiment. Nitrogen adsorption–desorption isotherms are obtained on an ASAP 2020 (Micromeritics Instruments, USA) nitrogen adsorption apparatus. All the samples are degassed at 60 °C prior to Brunauer–Emmett–Teller (BET) measurements. The BET specific surface area (S_{BET}) is determined by a multipoint BET method by using the adsorption data in the relative pressure P/P_0 range of 0.05–0.25. The desorption isotherm is used to determine the pore size distribution by using the Barret−Joyner−Halender method.[19] The nitrogen adsorption volume at $P/P_0 = 0.995$ is used to determine the pore volume and average pore size.

2.4. Measurement of Photocatalytic Activity. The evaluation of photocatalytic activity of the prepared samples for the photocatalytic decolorization of methyl orange aqueous solution is performed at ambient temperature, as reported in our previous studies.[20] Experimental procedures are as follows: 0.03 g of TiO_2 powder sample is dispersed in a 20 mL methyl orange aqueous solution with a concentration of 3.1×10^{-5} M in a dish with a diameter of about 9.0 cm. A 15 W, 365 nm UV lamp (Cole-Parmer Instrument Co.) is used as a light source, and the wavelength range of the UV lamp is about 220–440 nm. The average light intensity striking on the surface of the reaction solution is about 112 $\mu W\cdot cm^{-2}$, as measured by a UV meter (made in the photoelectric instrument factory of Beijing Normal University) with the peak intensity of 365 nm. The concentration of methyl orange is determined by an UV–visible spectrophotometer (UV-2550, Shimadzu, Japan). After UV irradiation for 30 min, the reaction solution is filtrated to measure the concentration change of the methyl orange. As the concentration of the methyl orange solution is very low, its photocatalytic decolorization process is a pseudo-first-order reaction and can be expressed as $\ln(c_0/c) = kt$, where k is the apparent rate constant and c_0 and c are the methyl orange concentrations at $t = 0$ and $t = t$, respectively.[20]

3. Results and Discussion

3.1. Morphology and Hierarchically Nanoporous Structure. Hierarchically nanoporous TiO_2 hollow microspheres are prepared via a simple one-step template-directed method (see Experimental Section). The XRD pattern (Figure 1) of the TiO_2 hollow spheres indicates that all peaks can be indexed as the anatase phase of TiO_2 (JCPDS No. 21-1272, space group $I4_1/amd$ (141)). According to the Scherrer equation, the average crystallite size is ca. 15 nm.

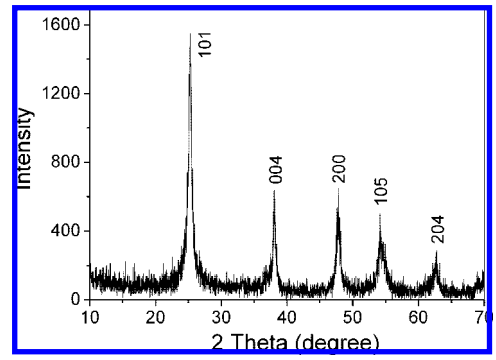

Figure 1. XRD pattern of TiO_2 hollow spheres obtained in a 0.02 M TiF_4 aqueous solution at 60 °C for 12 h.

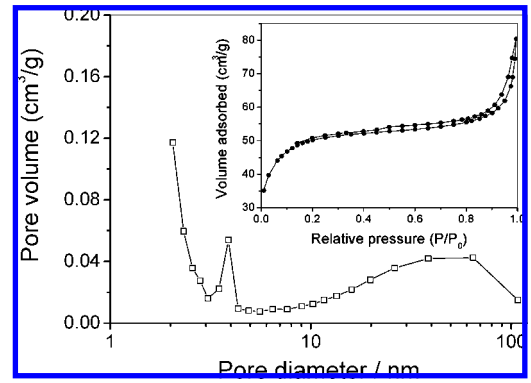

Figure 2. Nitrogen adsorption–desorption isotherm (inset) and corresponding pore-size distribution of TiO_2 hollow spheres obtained in a 0.02 M TiF_4 aqueous solution at 60 °C for 12 h.

The nitrogen adsorption–desorption isotherm (inset in Figure 2) of TiO_2 samples is a combination of types I and IV (BDDT classification). In a low relative pressure range (below 0.2), the isotherm exhibits a high adsorption, indicating the presence of micropores (type I),[19] implying that the samples still contain a small amount of amorphous TiO_2.[16] However, in the high relative pressure range of 0.4−1, the curve exhibits two small hysteresis loops, indicating bimodal pore-size distributions in the mesoporous and macroporous regions. The shapes of the two hysteresis loops are different from each other. At a low relative pressure, between 0.4 and 0.7, the hysteresis loop is of type H2, suggesting the existence of ink-bottle pores. However, at a high relative pressure, between 0.8 and 1.0, the hysteresis loop is of type H3, which is associated with slitlike pores.[19,21] The bimodal pore-size distribution is ascribed to two different pores: fine intra-aggregated pores formed between intra-agglomerated primary crystallites, and large inter-aggregated pores produced by inter-aggregated secondary particles.[21] This bimodal pore-size distribution is further confirmed by its corresponding pore-size distribution (Figure 2). Figure 2 indicates that the hollow microspheres contain micropores (below 2 nm), small mesopores (peak pore ca. 3.9 nm), and large mesopores and macropores (from 10 to 110 nm). These results demonstrate the existence of hierarchically nanoporous structures in the prepared samples on a multilength scale. The BET surface area of the TiO_2 hollow spheres is 174 m^2/g.

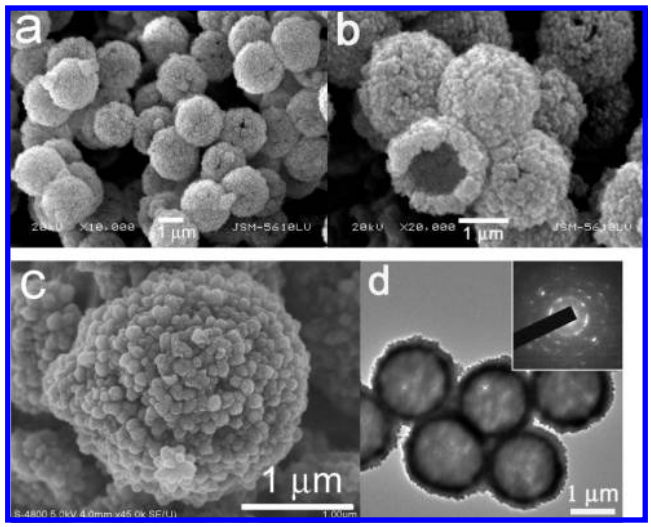

Figure 3. (a and b) SEM, (c) FESEM, and (d) TEM images of TiO_2 hollow spheres obtained in a 0.02 M TiF_4 aqueous solution at 60 °C for 12 h. Inset in (d) shows the SAED pattern of individual TiO_2 hollow sphere.

The hierarchically nanoporous structures of hollow spheres are further confirmed by their corresponding SEM and TEM images. A typical SEM image is shown in Figure 3a. It indicates that the TiO_2 hollow spheres have a narrow size distribution (average size ca. 2.2 μm). The high-magnification SEM images (Figure 3b,c) clearly show that the shells of the hollow spheres are composed of many small TiO_2 spherical particles with diameters of about 100 nm and appear to be higher-order porous superstructures. It should be emphasized that primary crystallites aggregate to form these small spherical particles and fine intra-aggregated pores (micropores to several-nanometer mesopores) within these particles.[22] The inter-aggregations or connections of these porous spherical particles result in the formation of larger inter-aggregated meso- and macropores in the range of 10−110 nm.[22] These aggregations or connections are due to the condensation reactions among the hydroxyl groups on the surface of adjacent porous spherical particles, which result in the formation of single hollow microspheres. These observations are in good agreement with the hierarchically porous structure of the hollow spheres, as revealed by the nitrogen adsorption analysis. The wall thickness of the TiO_2 hollow spheres is in the range of 300–350 nm, as shown in Figure 3b. Further observation shows that the as-prepared TiO_2 hollow spheres have smooth inner and rough external surfaces, suggesting that the formation of the TiO_2 hollow spheres is probably due to the template-directed deposition of TiO_2 nanoparticles on the surfaces of smooth SiO_2 spheres and in situ template-sacrificial dissolution.[11] The corresponding TEM image (Figure 3d) further confirms that all the microspheres consist of 1.5 μm hollow cavities and have a narrow size distribution. The selected area electron diffraction (SAED) pattern of the hollow spheres (inset in Figure 3d) reveals the polycrystalline nature of the anatase phase of the TiO_2 hollow spheres.

The chemical composition analysis, performed by using energy-dispersive X-ray spectroscopy (not shown here), indicates that the porous hollow microspheres are mainly composed of Ti, O, and F. These results are consistent with those from X-ray photoelectron spectroscopy (XPS) (Figure S2), in which Ti, O, F, and C are found in the microsphere sample and no Si element is observed, indicating the complete dissolution removal of SiO_2 microspheres.

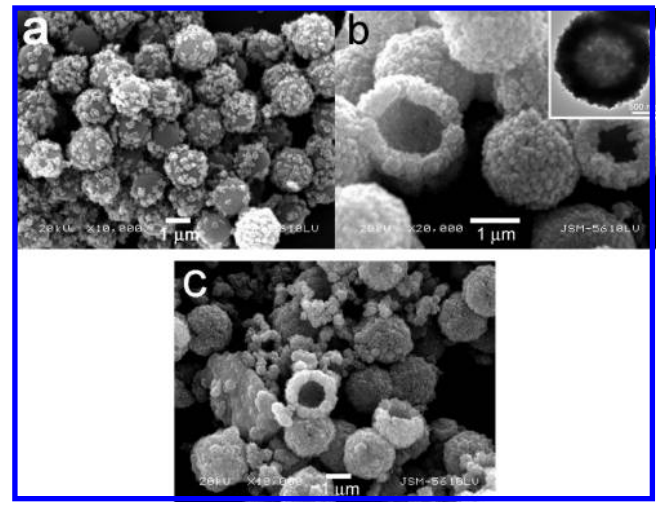

Figure 4. SEM images of the TiO_2 hollow spheres obtained in a (a) 0.01, (b) 0.06, and (c) 0.10 M TiF_4 aqueous solution. Inset in (b) shows the corresponding TEM image of sample (b).

The wall thickness of the TiO_2 hollow spheres can be easily tuned by adjusting the concentration of the precursor TiF_4. At a low TiF_4 concentration (0.01 M), the surface of the SiO_2 spherical template cannot be completely coated by the TiO_2 nanoparticles, and the SiO_2 template microspheres still remain in the products, probably because of the limited TiO_2 amount and HF concentration (Figure 4a). At a high TiF_4 concentration (0.06 M), the TiO_2 hollow spheres show thicker shells (about 380–430 nm) (Figure 4b and inset), implying that the wall thickness of the TiO_2 hollow spheres could be easily adjusted by changing the concentration of the precursor TiF_4. However, with a further increase of the TiF_4 concentration to 0.1 M, many ill-defined aggregates are observed in addition to the TiO_2 hollow spheres (Figure 4c) because of a high supersaturation. Further investigations show that the size of the TiO_2 hollow spheres can be easily adjusted by changing the size of the SiO_2 microspheres (not shown here).

3.2. Formation Mechanism. The formation mechanism of the hollow microspheres is investigated by TEM analysis of the structures isolated from the reaction mixture and maintained at 60 °C for various aging times. Prior to reaction (0 h), the SiO_2 microspheres show smooth surfaces and uniform sizes (1.5 μm) (Figure S1). After reaction for 1 h, some of the TiO_2 particles are randomly deposited on the surfaces of the SiO_2 microspheres via a heterogenerous nucleation and growth mechanism, while the size of the SiO_2 microsphere templates shows no obvious changes. With the increase of the reaction time, more TiO_2 particles further deposit on the surfaces of the SiO_2 templates or as-formed TiO_2 particles. After reaction for 5 h, in addition to the formation of TiO_2 shells, the size of SiO_2 spheres decreases significantly. This is attributed to the fact that the following hydrolysis and dissolution reactions exist in the reaction system:

$$TiF_4 + 4H_2O \rightarrow Ti(OH)_4 + 4HF \quad (1)$$

$$SiO_2 + 4HF \rightarrow SiF_4 + 2H_2O \quad (2)$$

Thus, the hydrolysis of TiF_4 leads to the production of HF. It is well-known that SiO_2 can be easily dissolved in a HF solution to form SiF_4. Therefore, with the increase of the reaction time and the continuous hydrolysis of TiF_4, the increasing concentration of HF results in the gradual dissolution of SiO_2 cores and the formation of TiO_2 hollow spheres with movable SiO_2 cores

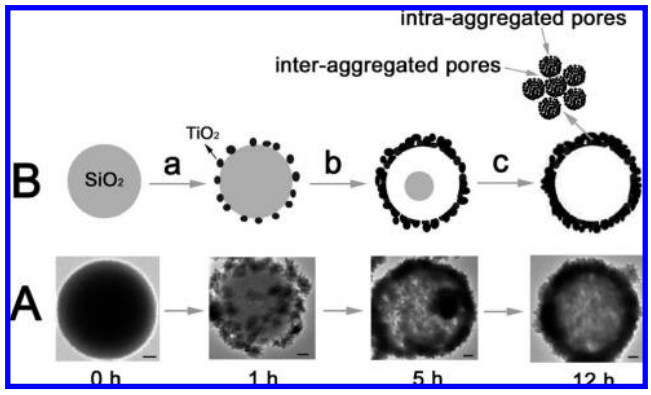

Figure 5. (a) TEM images of TiO_2 hollow spheres obtained in a 0.02 M TiF_4 aqueous solution at 60 °C for 0, 1, 5, and 12 h. (b) Schematic illustration of the formation of hierarchically nanoporous TiO_2 hollow spheres. The scale bar is 200 nm.

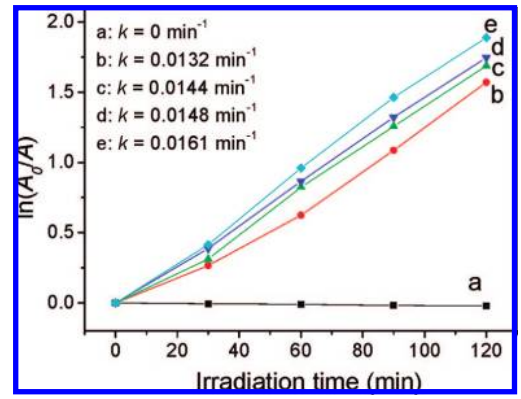

Figure 6. Plots of $\ln(A_0/A)$ versus irradiation time (t) for the TiO_2 hollow spheres obtained in a 0.02 M TiF_4 aqueous solution at 60 °C for 12 h. For comparison, the photocatalytic activity of P25 was also tested: (a) without photocatalyst, (b) P25 (without stirring), (c) P25 (with stirring), (d) 0.02 M (without stirring), and (e) 0.02 M (with stirring). The absorbance (A) on the y-axis is proportional to the concentration (c).

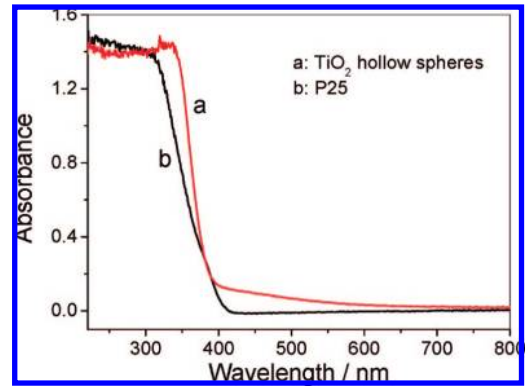

Figure 7. UV–visible spectra of the P25 and TiO_2 hollow microspheres obtained in a 0.02 M TiF_4 aqueous solution at 60 °C for 12 h.

inside. It is reasonable to conclude that the size of SiO_2 cores and shell thickness of TiO_2 hollow spheres can be controlled by adjusting the reaction time (such as 1 to 5 h). Obviously, the SiO_2/TiO_2 core–shell spherical structures can be easily prepared by this novel and simple method. With further increase of the reaction time to 12 h, the SiO_2 cores are completely dissolved by HF, which results in the formation of TiO_2 hollow spheres (Figure 5A). On the basis of the above TEM results, the formation of hierarchically porous TiO_2 hollow microspheres is illustrated in Figure 5B. First, titanium oxide primary sol particles deposit on the surface of the SiO_2 spheres by the slow hydrolysis and condensation of titanium tetrafluoride. These sol particles then agglomerate to produce micro- and mesoporous secondary spherical particles (Figure 5a). With increasing time, large meso- and macroporous particles are produced through the self-assembly of these secondary spherical particles. The SiO_2 templates are gradually dissolved because of the increase of the concentration of HF (Figure 5b). Moreover, the porous wall structures of the TiO_2 hollow spheres allow the continuous diffusion of ions until the SiO_2 microsphere templates are completely consumed, resulting in the formation of TiO_2 hollow spheres (Figure 5c). Therefore, it can be deduced that the formation of the TiO_2 hollow spheres is due to the template-directed deposition of TiO_2 nanoparticles and the in situ template-sacrificial dissolution of SiO_2 microspheres. The cavity size (1.5 μm) of hollow microspheres, commensurate with the diameter of the solid SiO_2 templates, and their smooth inner surfaces further confirm the above proposed formation mechanism.

The above results highlight a facile one-step low-temperature strategy for the fabrication of uniform hollow microspheres of crystalline TiO_2 (anatase) in high yield. The BET results, along with those from XRD, SEM, and TEM analyses, indicate that the hollow microspheres are composed of at least three levels of hierarchically porous structures: (i) fine intra-aggregated pores (less than several nanometers) due to the aggregation of primary particles, (ii) large inter-aggregated pores (10−110 nm) due to mesoscale packing of secondary aggregation particles in the shell wall, and (iii) assembly of a self-supporting, continuous outer shell enclosing an internal cavity space of about 1.5 μm.[16]

3.3. Photocatalytic Activity. The photocatalytic activities of the prepared TiO_2 samples and Degussa P25 TiO_2 powders (P25) are compared (Figure 6). Illumination in the absence of photocatalysts does not result in the photocatalytic decolorization of the methyl orange solution. On the contrary, the concentration of the methyl orange slightly increases because of the evaporation of H_2O in the reaction system. After the addition of TiO_2 photocatalysts, the concentration of the methyl orange decreases rapidly with increasing UV irradiation time. The linearity between $\ln(A_0/A)$ and t is good for all the TiO_2 samples. This further indicates the pseudo-first-order reaction of the photocatalytic degradation of methyl orange. The rate constants are calculated according to the slope of these lines, as shown in the Figure 6. Obviously, under stirring conditions, the photocatalysts show a higher photocatalytic activity than that of the same sample without stirring. Surprisingly, in the absence of stirring, our hierarchically nanoporous TiO_2 hollow microspheres exhibit a rate constant of 0.0148 min^{-1}, which is larger than that of P25 (k = 0.0132 min^{-1}). Moreover, under the stirring conditions, the photocatalytic activity of the TiO_2 hollow spheres further increases, and k reaches 0.0161 min^{-1}. The higher photocatalytic activity of the TiO_2 hollow micropsheres can be ascribed to the fact that the hollow sample has an unusual hierarchically nanoporous structure, which allows more effective transport for the reactant molecules to get to the active sites on the framework walls, hence, enhancing the efficiency of photocatalysis.[13,16] In previous studies, it was reported that the TiO_2 hollow spheres had a small band gap, resulting in the absorption in the long-wavelength region.[11c,d] To investigate the absorption properties of the TiO_2 hollow spheres, the UV–visible spectra of the TiO_2 hollow spheres were measured and are shown in Figure 7. It is found that the prepared TiO_2 hollow microspheres show a stronger absorption in the UV–visible region (310–700 nm) than P25. Thus, this also leads

to the enhanced photocatalytic activity of the TiO_2 hollow spheres. Similar results were also reported by Nakashima et al.[11c,d] However, the exact mechanism for the hollow-sphere structure to enhance the photocatalytic activity will be further investigated in future works.

Additional investigations show that the hollow microspheres can be readily separated from the slurry system by filtration or sedimentation after photocatalytic reaction and reused. Therefore, the prepared TiO_2 hollow spheres can be regarded as an ideal photocatalyst for environmental purification at industrial scale. To the best of our knowledge, this is the first time that the one-pot low-temperature preparation and photocatalytic activity of hierarchically nanoporous TiO_2 hollow spheres are reported. We believe that the prepared hierarchically nanoporous TiO_2 hollow microspheres are also of great interest for solar cells, catalysis, separation technology, biomedical engineering, and nanotechnology.

4. Conclusion

In summary, a simple one-step low-temperature template method has been developed to prepare hierarchically nanoporous hollow spheres of crystalline TiO_2. The wall thickness and size of the TiO_2 hollow spheres can be controlled by adjusting the experimental parameters, such as the concentration of the precursor TiF_4, the aging time, and the size of the SiO_2 spheres. The prepared samples show a high photocatalytic activity on the degradation of a methyl orange aqueous solution and can be readily separated from a slurry system after photocatalytic reaction. We think that these hierarchically porous nanocrystalline TiO_2 hollow spheres should have great applications in photocatalysis, catalysis, solar cells, and separation and purification processes.

Acknowledgment. This work was partially supported by the National Natural Science Foundation of China (20473059, 50625208, and 20773097). This work was also financially supported by the Key Research Project of Chinese Ministry of Education (No. 106114), the National Basic Research Program of China (2007CB613302), and the Program for Changjiang Scholars and Innovative Research Team in University (PCSIRT, No. IRT0547), Ministry of Education, China.

Supporting Information Available: Figures S1 and S2, showing SEM and TEM images of SiO_2 spheres and XPS survey spectrum of TiO_2 hollow spheres, respectively. This information is available free of charge via the Internet at http://pubs.acs.org.

References

(1) (a) Caruso, F.; Caruso, R. A.; Mohwald, H. *Science* **1998**, *282*, 1111. (b) Caruso, R. A.; Susha, A.; Caruso, F. *Chem. Mater.* **2001**, *13*, 400. (c) Caruso, F. *Adv. Mater.* **2001**, *13*, 740.

(2) Zhong, Z.; Yin, Y.; Gates, B.; Xia, Y. *Adv. Mater.* **2000**, *12*, 206.

(3) Fowler, C. E.; Khushalani, D.; Mann, S. *J. Mater. Chem.* **2001**, *11*, 1968.

(4) (a) Yin, Y. D.; Rioux, R. M.; Erdonmez, C. K.; Hughes, S.; Somorjai, G. A.; Alivisatos, A. P. *Science* **2004**, *304*, 711. (b) Fan, H. J.; Knez, M.; Scholz, R.; Nielsch, K.; Pippel, E.; Hesse, D.; Zacharias, M.; Gosele, U. *Nat. Mater.* **2006**, *5*, 627.

(5) (a) Zeng, H. C. *J. Mater. Chem.* **2006**, *16*, 649. (b) Yang, H. G.; Zeng, H. C. *J. Phys. Chem. B* **2004**, *108*, 3492.

(6) (a) Sun, X. M.; Li, Y. D. *Angew. Chem., Int. Ed.* **2004**, *43*, 3827. (b) Sun, X. M.; Liu, J. F.; Li, Y. D. *Chem. Eur. J.* **2006**, *12*, 2039.

(7) Caruso, F. *Chem. Eur. J.* **2000**, *6*, 413.

(8) (a) Sun, Y. G.; Mayers, B.; Xia, Y. N. *Adv. Mater.* **2003**, *15*, 641. (b) Huang, J. X.; Xie, Y.; Li, B.; Liu, Y.; Qian, Y. T.; Zhang, S. Y. *Adv. Mater.* **2000**, *12*, 808.

(9) (a) Yu, J. G.; Guo, H. T.; Davis, S. A.; Mann, S. *Adv. Funct. Mater.* **2006**, *16*, 2035. (b) Yu, H. G.; Yu, J. G.; Liu, S. W.; Mann, S. *Chem. Mater.* **2007**, *19*, 4327.

(10) (a) Muthusamy, E.; Walsh, D.; Mann, S. *Adv. Mater.* **2002**, *14*, 969. (b) Strohm, H.; Lobmann, P. *Chem. Mater.* **2005**, *17*, 6772. (c) Strohm, H.; Lobmann, P. *J. Mater. Chem.* **2004**, *14*, 138. (d) Nakashima, T.; Kimizuka, N. *J. Am. Chem. Soc.* **2003**, *125*, 6386. (e) Jung, J. H.; Kobayashi, H.; van Bommel, K. J. C.; Shinkai, S.; Shimizu, T. *Chem. Mater.* **2002**, *14*, 1445. (f) Yu, H. G.; Yu, J. G.; Cheng, B.; Liu, S. W. *Nanotechnology* **2007**, *18*, 065604.

(11) (a) Li, H.; Bian, Z.; Zhu, J.; Zhang, D.; Li, G.; Huo, Y.; Li, H.; Lu, Y. *J. Am. Chem. Soc.* **2007**, *129*, 8406. (b) Yu, J. G.; Liu, S. W.; Yu, H. G. *J. Catal.* **2007**, *249*, 59. (c) Syoufian, A.; Satriya, O. H.; Nakashima, K. *Catal. Commun.* **2007**, *8*, 755. (d) Syoufian, A.; Nakashima, K. *J. Colloid Interface Sci.* **2007**, *313*, 213.

(12) (a) Peng, Q.; Xu, S.; Zhuang, Z.; Wang, X.; Li, Y. *Small* **2005**, *1*, 216. (b) Nishimura, S.; Abrams, N.; Lewis, B. A.; Halaoui, L. I.; Mallouk, T. E.; Benkstein, K. D.; van de Lagemaat, J.; Frank, A. J *J. Am. Chem. Soc.* **2003**, *125*, 6306.

(13) (a) Wang, X. C.; Yu, J. C.; Ho, C. M.; Hou, Y. D.; Fu, X. Z. *Langmuir* **2005**, *21*, 2552. (b) Ho, W.; Yu, J. C.; Lee, S. *Chem. Commun.* **2006**, 1115. (c) Yu, J. G.; Yu, H. G.; Cheng, B.; Zhao, X. J.; Zhang, Q. J. *J. Photochem. Photobiol. A* **2006**, *182*, 121.

(14) (a) Yuan, Z. Y.; Su, B. L. *J. Mater. Chem.* **2006**, *16*, 663. (b) Blin, J. L.; Leonard, A.; Yuan, Z. Y.; Gigot, L.; Vantomme, A.; Cheetham, A. K.; Su, B. L. *Angew. Chem., Int. Ed.* **2003**, *42*, 2872.

(15) Collins, A.; Carriazo, D.; Davis, S. A.; Mann, S. *Chem. Commun.* **2004**, 568.

(16) (a) Yu, J. G.; Su, Y. R.; Cheng, B. *Adv. Funct. Mater.* **2007**, *17*, 1984. (b) Yu, J. G.; Zhang, L. J.; Cheng, B.; Su, Y. R. *J. Phys. Chem. C* **2007**, *111*, 10582.

(17) Coppens, M. O.; Sun, J.; Maschmeyer, T. *Catal. Today* **2001**, *69*, 331.

(18) (a) Zhao, L.; Yu, J. G.; Cheng, B.; Yu, C. Z. *J. Non-Cryst. Solids* **2005**, *351*, 3593. (b) Zhao, L.; Yu, J. G.; Cheng, B. *J. Solid State Chem.* **2005**, *178*, 1818.

(19) Sing, K. S. W.; Everett, D. H.; Haul, R. A. W.; Moscou, L.; Pierotti, R. A.; Rouquerol, J.; Siemieniewska, T. *Pure Appl. Chem.* **1985**, *57*, 603.

(20) (a) Yu, J. G.; Yu, H. G.; Cheng, B.; Zhao, X. J.; Yu, J. C.; Ho, W. K. *J. Phys. Chem. B* **2003**, *107*, 13871. (b) Yu, J. G.; Yu, H. G.; Ao, C. H.; Lee, S. C.; Yu, J. C.; Ho, W. K. *Thin Solid Films* **2006**, *496*, 273.

(21) (a) Yu, J. G.; Yu, J. C.; Leung, M. K. P.; Ho, W. K.; Cheng, B.; Zhao, X. J.; Zhao, J. C. *J. Catal.* **2003**, *217*, 69. (b) Yu, J. G.; Yu, J. C.; Ho, W. K.; Leung, M. K. P.; Cheng, B.; Zhang, G. K.; Zhao, X. J. *Appl. Catal., A* **2003**, *255*, 309.

(22) (a) Yu, J. G.; Wang, G. H.; Cheng, B.; Zhou, M. H. *Appl. Catal., B* **2007**, *69*, 171. (b) Yu, J. G.; Su, Y. R.; Cheng, B.; Zhou, M. H. *J. Mol. Catal. A: Chem.* **2006**, *258*, 104.

CG700794Y